



Contents lists available at ScienceDirect

European Journal of Medicinal Chemistry

journal homepage: <http://www.elsevier.com/locate/ejmech>

Research paper

New (aryllalkyl)azole derivatives showing anticonvulsant effects could have VGSC and/or GABA_AR affinity according to molecular modeling studiesSuat Sari^a, Arzu Karakurt^{b,*}, Harun Uslu^b, F. Betül Kaynak^c, Ünsal Çalıř^a, Sevim Dalkara^a^a Hacettepe University, Faculty of Pharmacy, Department of Pharmaceutical Chemistry, 06100, Ankara, Turkey^b İnönü University, Faculty of Pharmacy, Department of Pharmaceutical Chemistry, 44280, Malatya, Turkey^c Hacettepe University, Faculty of Engineering, Department of Physics Engineering, 06532, Ankara, Turkey

ARTICLE INFO

Article history:

Received 23 May 2016

Received in revised form

11 July 2016

Accepted 14 August 2016

Available online 25 August 2016

Keywords:

(Aryllalkyl)azole

Anticonvulsant

Voltage gated sodium channel

A-type GABA receptor

Molecular docking

X-ray crystallography

Microwave chemistry

ABSTRACT

(Aryllalkyl)azoles (AAAs) emerged as a novel class of antiepileptic agents with the invention of nafimidone and denzimol. Several AAA derivatives with potent anticonvulsant activities have been reported so far, however neurotoxicity was usually an issue. We prepared a set of ester derivatives of 1-(2-naphthyl)-2-(1H-1,2,4-triazol-1-yl)ethanone oxime and evaluated their anticonvulsant and neurotoxic effects in mice. Most of our compounds were protective against maximal electroshock (MES)- and/or subcutaneous metrazol (s.c. MET)-induced seizures whereas none of them showed neurotoxicity. Nafimidone and denzimol have an activity profile similar to that of phenytoin or carbamazepine, both of which are known to inhibit voltage-gated sodium channels (VGSCs) as well as to enhance γ -aminobutyric acid (GABA)-mediated response. In order to get insights into the effects of our compounds on VGSCs and A-type GABA receptors (GABA_AR) we performed docking studies using homology model of Na⁺ channel inner pore and GABA_AR as docking scaffolds. We found that our compounds bind VGSCs in similar ways as phenytoin, carbamazepine, and lamotrigine. They showed strong affinity to benzodiazepine (BZD) binding site and their binding interactions were mainly complied with the experimental data and the reported BZD binding model.

© 2016 Elsevier Masson SAS. All rights reserved.

1. Introduction

Epilepsy is a chronic neurological disorder, which disrupts social and labour life, inflicting 1 in every 26 people [1]. The toll epilepsy takes is even heavier in developing countries [2]. Epilepsy usually starts in early childhood and lasts for a lifetime. Without a radical cure available, patients are obliged to take medication for years thus exposed to severe side effects, drug-drug interactions, and

long term toxicity. Furthermore, currently available antiepileptic drugs (AEDs) fail to achieve adequate seizure control in one third of the patients [3]. That is why the need for new AEDs that are safe, selective, and more effective is urgent.

(Aryllalkyl)azoles (AAAs) emerged as a novel class of antiepileptic agents with nafimidone and denzimol (Fig. 1) [4,5]. They possess an activity profile similar to that of phenytoin and carbamazepine, which act through voltage-gated sodium channels (VGSCs) inhibition although these drugs were reported to enhance γ -aminobutyric acid (GABA)-mediated response, as well [6,7]. Structure-activity relationship (SAR) studies on AAAs have revealed that an aromatic ring, an azole (usually imidazole and 1,2,4-triazole) group, and an alkyl chain of two-carbon long connecting these two are necessary for high anticonvulsant activity. These studies point out the essence of a small oxygen functional group (such as carbonyl, ethylene dioxy, methoxy, acyloxy, hydroxy, and oxime ether moieties) attached to the alkyl bridge for a better anticonvulsant activity, as well [8,9].

Abbreviations: AAA, (aryllalkyl)azole; MES, maximal electroshock; s. c. MET, subcutaneous metrazol; VGSC, voltage-gated sodium channel; GABA, γ -aminobutyric acid; GABA_AR, A-type GABA receptor; BZD, benzodiazepine; AED, antiepileptic drug; SAR, structure-activity relationship; MW, microwave; MM, molecular mass; MP, melting point; DCC, *N,N'*-dicyclohexylcarbodiimide; DMAP, 4-dimethylaminopyridine; LA, local anaesthetic.

* Corresponding author.

E-mail addresses: arzu.karakurt@inonu.edu.tr, arzukarakurt@hotmail.com (A. Karakurt).<http://dx.doi.org/10.1016/j.ejmech.2016.08.032>

0223-5234/© 2016 Elsevier Masson SAS. All rights reserved.

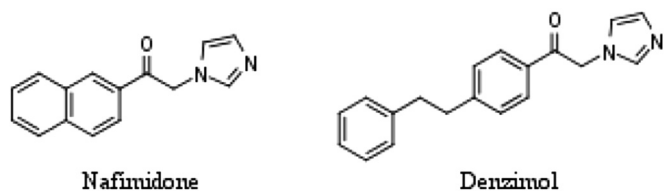


Fig. 1. Chemical structure of nafimidone and denzimol.

Previously, Karakurt et al. prepared several oxime ether derivatives of 1-(2-naphthyl)-2-(1*H*-1,2,4-triazol-1-yl)ethanone [10], carboxylic ester derivatives of nafimidone alcohol [11], and oxime ester derivatives of nafimidone [12], some of which proved highly protective against convulsions in test animals.

In the light of these facts, we prepared 14 novel 1-(2-naphthyl)-2-(1*H*-1,2,4-triazol-1-yl)ethanone oxime ester derivatives through modifications on the oxime ester function and evaluated their anticonvulsant and neurotoxic effects in mice using maximal electroshock (MES), subcutaneous metrazol (s.c. MET), and rotarod tests. Microwave (MW) irradiation was applied during synthesis of the synthons, by which the amount of time required was greatly reduced and the yields were increased [13].

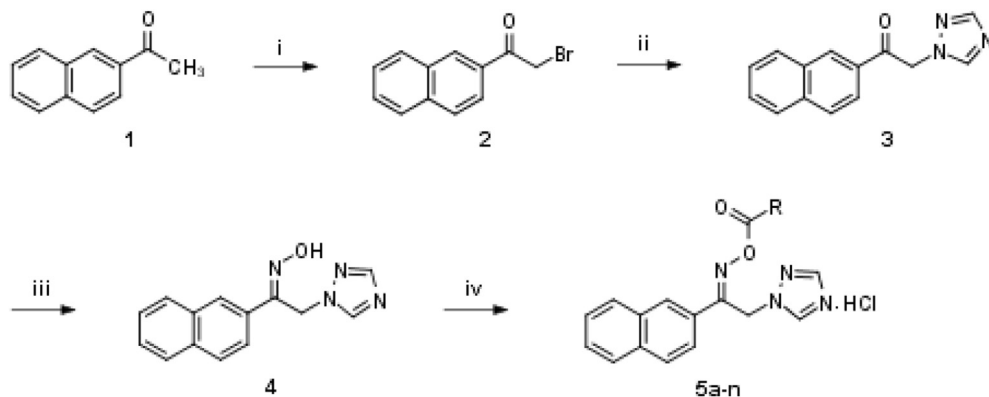
In order to test whether our compounds could act through VGSCs and/or A-type GABA receptors (GABA_ARs), which account for the principal mechanisms of action for many AEDs [9], and understand their possible interactions with these targets we performed docking studies on an open (activated) Na⁺ channel inner pore [14] and a native GABA_AR model [15].

2. Results and discussion

2.1. Chemistry

As outlined in Scheme 1, 1-bromo-2-(2-naphthyl)ethanone (**2**) was prepared by the reported method [16]. Sodium salt of 1,2,4-1*H*-triazole was alkylated with **2** to yield 1-(2-naphthyl)-2-(1*H*-1,2,4-triazol-1-yl)ethanone (**3**) [17]. **3** was then converted to its oxime derivative (**4**) using NH₂OH.HCl in strong basic medium (pH: 14) [18]. **3** and **4** were effected via MW irradiation [13], which saved reasonable time and increased yield regarding conventional methods (Table 1).

Final compounds (**5a-n**) were synthesized by the Steglich esterification [19] of **4** with proper carboxylic acids or anhydrides in the presence of *N,N*'-dicyclohexylcarbodiimide (DCC) and 4-dimethylaminopyridine (DMAP) in dichloromethane (DCM); by



Scheme 1. (1.5 column). Reagents and conditions: (i) Br₂, CH₃COOH, 0–5 °C; (ii) 1*H*-1,2,4-triazole, Na⁺, CH₃OH, MW 70 °C, 500 W; (iii) NH₂OH.HCl, C₂H₅OH, pH 14, MW 70 °C, 500 W; (iv) DCC, DMAP, DCM, gHCl.

Table 1
MW irradiation conditions of **3** and **4** in comparison with conventional reaction conditions.

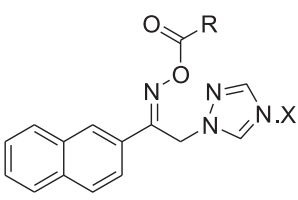
Comp.	MW irradiation method		Conventional method	
	Time (min.)	Yield (%)	Time (min.)	Yield (%)
3	16	98	360	59
4	8	85	180	78.

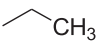
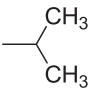
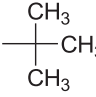
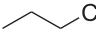
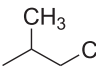
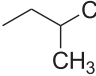
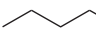
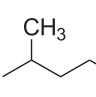
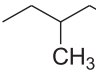
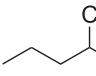
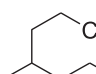
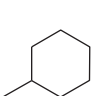
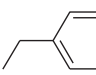
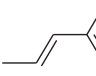
this way structural modifications were applied on “R” moiety (Table 2). They were purified by column chromatography and/or crystallization. **5a**, **5b**, **5f-k**, and **5m** were converted to their HCl salts with gaseous HCl (gHCl). Their structures were confirmed by IR, ¹H NMR, mass spectra, and elemental analysis.

4 was established by X-ray crystallographic analysis and proved to be in *Z* configuration (Fig. 2A). It was crystallized under a non-centrosymmetric orthorhombic structure with space group Pc21n and its unit cell dimensions were found to be: *a* = 5.1237(3) Å, *b* = 10.9258(8) Å and *c* = 21.8692(17) Å, *Z* = 4. The naphthyl moiety is almost planar and makes an angle 71.09° with the triazole ring. The packing of the molecules and the hydrogen bonding in the structure are shown in Fig. 2B. The X-ray structure contains strong O/H...N inter-molecular H-bond interaction [O1...H1A 2.6897 Å, O1-H1A 0.82 Å and O1...H1A-N3 168°] by Platon program [20]. O/H...N interaction contributes to the formation of chains in zig-zag configuration along *b* direction [symmetry code: −1/2+*x*, −1/2+*y*, 1/2−*z*]. There is also a strong C12/H12 ... Cg2 (1+*x*, *y*, *z*) interaction which stabilizes the crystal packing (H ... Cg2: of 2.90 Å).

Previously, certain oxime ethers derivatives were reported to be in the same configuration with their oxime precursors [22]. Accordingly, we expected **5a-n** to be in *Z* configuration however in the ¹H NMR spectra of the most of our compounds we observed signals of both diastereomers in varying intensities. These signals were detectable for the protons of the methylene next to the triazole ring (−CH₂−N), the triazole protons, and the protons belong to the oxime ester group. For instance, the −CH₂−N protons of **5f** next to the triazole ring were observed as two singlets, an upfield peak (5.81 ppm) of 31% intensity and a downfield peak (5.90 ppm) of 69%. These percentages were very close for each proton or set of protons of the other affected groups on the molecule. The chemical shifts and intensities of the methylene protons of each diastereomer for compounds that show mixture of diastereomers in their ¹H NMR spectra are given in Table 2. One reason for the occurrence of a mixture of diastereomers in ¹H NMR spectra of these compounds could be interconversion of diastereomers due to heating during NMR run [23]. Previously *E* and *Z* isomers of 1-(2-naphthyl)-

Table 2
Structures, molecular masses, yields, melting points, and $\log P$ values of **5a–n**.



Comp.	R	X	MM ^a (g/mol)	Yield (%)	MP ^b (°C)	$\log P$
5a		HCl	308.34	39	138–40	2.89
5b		HCl	322.37	44	134–6	3.13
5c		–	336.39	42	131–2	3.71
5d		–	322.37	39	119–21	3.45
5e		–	336.39	31	109–10	3.64
5f		HCl	336.39	29	129–30	3.66
5g		HCl	336.39	49	130–2	3.95
5h		HCl	350.42	79	127–9	4.20
5i		HCl	350.42	71	122–5	3.91
5j		HCl	350.42	72	127–30	3.93
5k		HCl	378.48	82	135–8	5.26
5l		–	362.43	53	145–7	4.30
5m		HCl	370.41	35	126–9	3.81
5n		–	382.42	26	162	4.36

^a Molecular mass.

^b Melting point.

2-(imidazol-1-yl)ethanone-*O*-ethyl oxime were separately isolated and in their ¹H NMR spectra, the –CH₂-N protons of the *Z* isomer of this compound were observed to resonate at higher frequency than those of the *E* isomer [24]. Therefore we speculate that the down-field signals in Table 3, which occur at higher intensities, belong to the *Z* isomers.

We tested drug-likeness of our compounds using MLViS, a web tool which makes use of 10 machine-learning methods selected

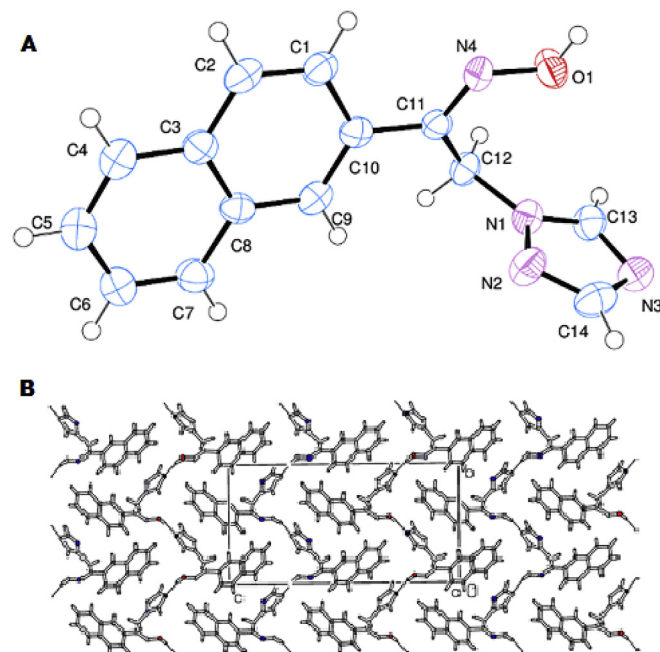


Fig. 2. The ORTEP 3 [21] (A) and packing diagram (B) of **4**. Displacement ellipsoids are drawn at the 50% probability level. Hydrogen atoms are shown as spheres of arbitrary radius.

Table 3

Chemical shifts of –CH₂-N protons of each diastereomer and their relative intensities for compounds ¹H NMR spectra of which show diastereomer mixtures.

Comp.	<i>E</i>		<i>Z</i>	
	Chemical shift (ppm)	Intensity %	Chemical shift (ppm)	Intensity %
5a	5.61	37	5.70	63
5b	5.56	49	5.67	51
5d	5.50	5	5.65	95
5f	5.81	31	5.90	69
5g	5.78	30	5.86	70
5h	5.80	35	5.88	65
5i	5.91	35	6.00	65
5j	5.83	33	5.92	67
5k	5.90	44	6.01	56

among 23 algorithms based on principal component and hierarchical cluster analysis results to predict drug-likeness [25]. The tool uses six molecular descriptors ($\log P$, polar surface area, hydrogen donor count, aliphatic ring count, aromatic ring count, and Balaban Index) as input, which were previously reported to be the best among 34 features [26]. 12 compounds were found drug-like according to the algorithms provided by MLViS (Table 4). **5m** and **5n** were found nondrug-like in two kernel-based methods (IsSVMrbf, SVMrbf), kNN, an instance-based learning algorithm, and neural networks (NN) algorithm.

2.2. Pharmacology

10 Compounds among **5a–n** showed protection in either or both of the tests at one of the given doses and periods at least. More compounds were protective against MES-induced seizures than s.c. MET-induced seizures, which usually is the case for AAAs [10,11,24]. Those active against MES-induced seizures were protective mostly up to 0.5 h. However those s.c. MET-active were protective up to 4 h but at 300 mg/kg except for **5f**, which was the only derivative to show protection at 30 mg/kg **5m** and **5n**, which were inactive,

Table 4
Drug-likeness of **5a-n** according to MLViS web tool.

Comp.	FDA ^a	C5	J48	lsSVMrbf ^b	SVMrbf ^c	SVMlin ^d	RF ^e	Bag SVM ^f	kNN ^g	NN ^h
5a	Drug-like	Drug-like	Drug-like	Drug-like	Drug-like	Drug-like	Drug-like	Drug-like	Drug-like	Drug-like
5b	Drug-like	Drug-like	Drug-like	Drug-like	Drug-like	Drug-like	Drug-like	Drug-like	Drug-like	Drug-like
5c	Drug-like	Drug-like	Drug-like	Drug-like	Drug-like	Drug-like	Drug-like	Drug-like	Drug-like	Drug-like
5d	Drug-like	Drug-like	Drug-like	Drug-like	Drug-like	Drug-like	Drug-like	Drug-like	Drug-like	Drug-like
5e	Drug-like	Drug-like	Drug-like	Drug-like	Drug-like	Drug-like	Drug-like	Drug-like	Drug-like	Drug-like
5f	Drug-like	Drug-like	Drug-like	Drug-like	Drug-like	Drug-like	Drug-like	Drug-like	Drug-like	Drug-like
5g	Drug-like	Drug-like	Drug-like	Drug-like	Drug-like	Drug-like	Drug-like	Drug-like	Drug-like	Drug-like
5h	Drug-like	Drug-like	Drug-like	Drug-like	Drug-like	Drug-like	Drug-like	Drug-like	Drug-like	Drug-like
5i	Drug-like	Drug-like	Drug-like	Drug-like	Drug-like	Drug-like	Drug-like	Drug-like	Drug-like	Drug-like
5j	Drug-like	Drug-like	Drug-like	Drug-like	Drug-like	Drug-like	Drug-like	Drug-like	Drug-like	Drug-like
5k	Drug-like	Drug-like	Drug-like	Drug-like	Drug-like	Drug-like	Drug-like	Drug-like	Drug-like	Drug-like
5l	Drug-like	Drug-like	Drug-like	Drug-like	Drug-like	Drug-like	Drug-like	Drug-like	Drug-like	Drug-like
5m	Drug-like	Drug-like	Drug-like	Nondrug-like	Nondrug-like	Drug-like	Drug-like	Drug-like	Drug-like	Nondrug-like
5n	Drug-like	Drug-like	Drug-like	Nondrug-like	Nondrug-like	Drug-like	Drug-like	Drug-like	Nondrug-like	Nondrug-like

^a Flexible Discriminant Analysis.

^b Least Squares Support Vector Machines with Radial Basis Function.

^c Support Vector Machines with Radial Basis Function.

^d Support Vector Machines with Linear Kernel Function.

^e Random Forests.

^f Bagged Support Vector Machines with Radial Basis Function.

^g k-Nearest Neighbours.

^h Neural Networks.

Table 5
Anticonvulsant and neurotoxicity screening results of **5a-n** and reference AEDs (The data indicating observed activity/toxicity is highlighted as bold.).

Screen	Time (h)	Dose (mg/kg)	5a	5b	5c	5d	5e	5f	5g	5h	5i	5j	5k	5l	5m	5n	Phe. ^a	Carb. ^b	
MES^c	0.5	30	0/1	0/1	0/1	0/1	0/1	0/1	0/1	0/1	0/1	0/1	0/1	0/1	0/1	0/1	1/1	1/1	
		100	0/1	0/1	0/1	0/1	1/1	0/1	0/1	0/1	1/1	1/1	0/1	0/1	0/1	0/1	1/1	1/1	
		300	0/1	0/1	0/1	0/1	1/1	1/1	1/1	1/1	0/1	1/1	0/1	1/1	–	0/1	1/1	1/1	
	4	30	0/1	0/1	0/1	0/1	0/1	0/1	0/1	0/1	0/1	0/1	0/1	0/1	0/1	0/1	0/1	1/1	0/1
		100	0/1	0/1	0/1	0/1	0/1	1/1	0/1	0/1	0/1	0/1	0/1	0/1	0/1	0/1	0/1	1/1	1/1
		300	0/1	1/1	0/1	1/1	0/1	0/1	0/1	0/1	0/1	1/1	0/1	1/1	0/1	0/1	0/1	1/1	1/1
s.c. MET^d	0.5	30	0/1	0/1	0/1	0/1	0/1	0/1	0/1	0/1	0/1	0/1	0/1	0/1	0/1	0/1	0/1	0/1	
		100	0/1	0/1	0/1	0/1	0/1	0/1	0/1	0/1	0/1	0/1	0/1	0/1	0/1	0/1	0/1	0/1	
		300	0/1	0/1	0/1	0/1	0/1	1/1	0/1	0/1	0/1	0/1	0/1	0/1	0/1	0/1	0/1	0/1	
	4	30	0/1	0/1	0/1	0/1	0/1	0/1	1/1	0/1	0/1	0/1	0/1	0/1	0/1	0/1	0/1	0/1	0/1
		100	0/1	0/1	0/1	0/1	0/1	0/1	1/1	0/1	0/1	0/1	0/1	0/1	0/1	0/1	0/1	0/1	1/1
		300	0/1	0/1	0/1	0/1	1/1	1/1	0/1	0/1	0/1	1/1	1/1	1/1	0/1	0/1	0/1	0/1	1/1
TOX^e	0.5	30	0/2	0/2	0/2	0/2	0/2	0/2	0/2	0/2	0/2	0/2	0/2	0/2	0/2	0/2	0/2	0/2	
		100	0/2	0/2	0/2	0/2	0/2	0/2	0/2	0/2	0/2	0/2	0/2	0/2	0/2	0/2	0/2	0/2	
		300	0/2	0/2	0/2	0/2	0/2	0/2	0/2	0/2	0/2	0/2	0/2	0/2	0/2	0/2	0/1	2/2	2/2
	4	30	0/2	0/2	0/2	0/2	0/2	0/2	0/2	0/2	0/2	0/2	0/2	0/2	0/2	0/2	0/2	0/2	0/2
		100	0/2	0/2	0/2	0/2	0/2	0/2	0/2	0/2	0/2	0/2	0/2	0/2	0/2	0/2	0/2	2/2	2/2
		300	0/2	0/2	0/2	0/2	0/2	0/2	0/2	0/2	0/2	0/2	0/2	0/2	0/2	0/2	0/2	2/2	0/2

^a Phenytoin.

^b Carbamazepine.

^c Maximal electroshock (number of mice protected/number of mice tested).

^d Subcutaneous metrazol (number of mice protected/number of mice tested).

^e Neurotoxicity (number of mice failed rotarod test/number of mice tested).

proved nondrug-like in some of the algorithms of MLViS web tool. These were the only derivatives with an aryl group on the oxime ester function. Taken together, it is not possible to establish SARs for these compounds regarding the modifications on the oxime ester group. On the other hand, relatively high *clogP* values might be one of the factors behind the lack of anticonvulsant efficacy at lower doses because high lipophilicity might cause issues such as metabolism, solubility, deposition in adipose tissues, and plasma protein binding. We did not observe any sign of neurotoxicity with any of the compounds unlike previously reported AAAs, which usually exhibit both protection and neurotoxicity at higher doses [10–12,24,27]. Anticonvulsant and neurotoxicity screening results of **5a-n** are presented in Table 5.

2.3. Molecular docking studies

VGSCs are transmembrane protein complexes that conduct Na⁺

through cell membrane in order to generate action potentials in neurons and muscle cells. They have a large pore forming alpha subunit which consists of four repeated domains (DI to DIV). Each domain has six transmembrane helices, labelled S1 to S6, and are assembled around the inner pore. VGSCs exist at three different states (closed, open, and inactivated). With increasing membrane potential the activation gate opens and the pore moves from closed (deactivated) to open (activated) state to conduct Na⁺, but at the highest membrane potential the inactivation gate closes and the channel becomes inactivated [28].

A member of the cys-loop receptor superfamily, GABA_ARs are responsible from the inhibitory postsynaptic potentials in central nervous system. When activated, a GABA_AR conducts Cl⁻ selectively through a central pore formed by its five subunits. Each subunit consists of an extracellular, transmembrane, and intracellular domain [29]. VGSCs and GABA_ARs are primary targets for many first-line AEDs [9,30]. Previously Lipkind and Fozzard [14] modelled

an open Na^+ channel inner pore composed of S5 and S6 residues. Through molecular docking they investigated binding modes and affinities of some local anaesthetics (LAs) and three AEDs that inhibit VGSCs (phenytoin, carbamazepine, and lamotrigine) which show higher affinity to the open/inactivated states of neuronal Na^+ channels [14,31]. They found that Phe-1764 and Tyr-1771 of DIV-S6 and Leu-1465 of DIII-S6 were key residues for binding affinities of these AEDs, in accordance with previous biological studies [32–34]. Bergman et al. [15] reported a unified model of GABA_AR of $\alpha_1\beta_2\gamma_2$ subunit composition and elucidated agonist and positive allosteric modulator binding through docking studies in the light of site directed mutagenesis data. We used the phenytoin bound VGSC inner pore model and the GABA and diazepam-bound GABA_AR model to perform docking studies of our four active derivatives, **5e**, **5f**, **5j**, **5l**, and one inactive, **5a**, on Glide, version 6.9, Schrödinger, LLC, New York, NY, 2015 [35–37].

2.3.1. VGSC docking

We docked our compounds into the wide mouth located between the selectivity filter and the activation gate, which is available only in the channel's open conformation, where some LAs, and the three AEDs, phenytoin, carbamazepine, and lamotrigine, were suggested to bind [14,31,33].

The binding mode of **5f** showed striking similarities to those previously obtained for the three AEDs, and its interactions with the active site residues were in accordance with the experimental data [14,31–34]. The naphthyl ring of **5f** engaged in strong aromatic π - π stacking and hydrophobic interactions with Phe-1764 and Tyr-1771 side chains, while the methylene group between the oxime and triazole had hydrophobic contacts with Leu-1465 side chain of DIII-S6 (Fig. 3).

The naphthyl ring occupied the same space as the phenyl of phenytoin in the proximity of DIV-S6 residues while the bulky isobutyl moiety faced the pore just like the other phenyl of phenytoin, suggested to block Na^+ conductance in the study of Lipkind and Fozzard [14]. The triazole lied towards cytosol making aromatic π - π interactions with the side chain of DIII-S6 Phe-1468 and the carbonyl oxygen was observed to make H-bond with the hydroxyl side chain of Thr-1464 of DIII-S6.

Positioned in the centre of channel lumen, the isobutyl moiety of **5f** had weak hydrophobic interactions with the side chains of DII-S6 residues, however these interactions, along with the strong hydrophobic and electrostatic interactions with DIV-S6 residues, might have stabilizing effect on the molecule in the central cavity. Lack of evidence on the importance DII-S6 residues for

ligand binding limits suggestions on the effects of "R" groups of our compounds on possible VGSC inhibition. On the other hand it is plausible to propose that too large an "R" group would render the compound unable to infiltrate into the inner pore. **5f** and other derivatives do not have heteroatom-bound hydrogen thus lacked so-called aromatic-H bond observed between the nitrogen-bound hydrogens of the three AEDs and Phe-1764 phenyl ring, which was suggested to be a key feature for voltage dependent VGSC inhibition of these drugs [14]. It was also argued that the alkylamine heads of aminoamide type LAs like lidocaine, since protonated in physiological pH, created a positive electrostatic barrier for Na^+ passage [31]. This was not the case in our study because our derivatives are non-ionized in physiological pH. Thus we suggest that **5f** could sterically occlude the inner pore blocking Na^+ influx with its bulky naphthalene and isobutyl groups (Fig. 4), in a similar way the three AEDs were suggested to do [14].

Docking of **5e**, **5j**, and **5l** yielded similar poses and interactions to those of **5f** (Fig. 5), except that the binding mode of **5l** differed from the others in that it did not have H-bond with Thr-1464, but had a weak H-bond between one of its aromatic hydrogens on the naphthalene ring and DIV-S6 Val-1767 carbonyl oxygen and its triazole ring did not interact with Phe-1468. **5e** has a chiral centre thus we took both enantiomers into consideration only to find they did not exhibit significant difference in binding interactions and

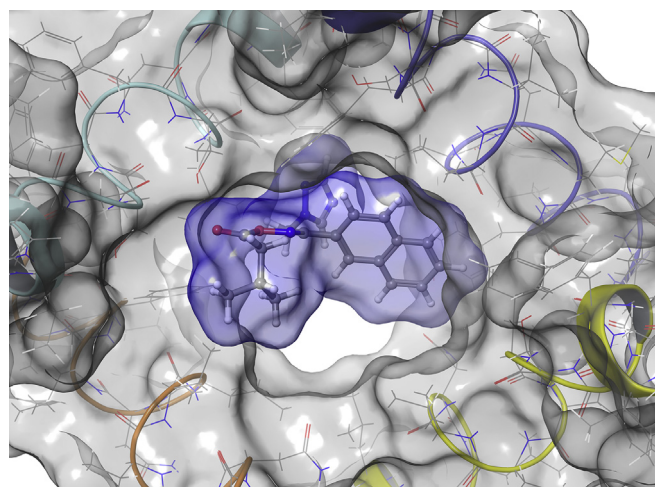


Fig. 4. Docking conformation of **5f** in the active site of Na^+ channel inner pore model (top view). Molecular surface of ligand and protein are rendered.

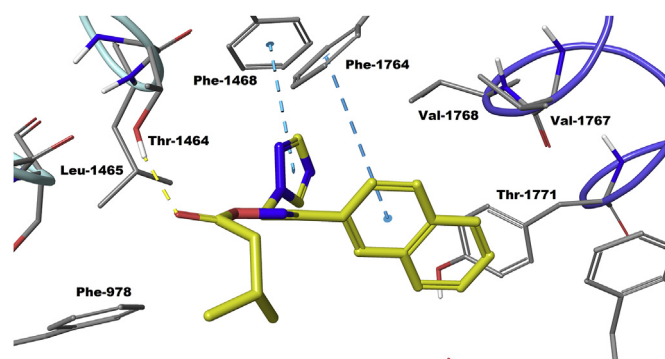


Fig. 3. Docking conformation of **5f** in the active site of Na^+ channel inner pore (top view). **5f** is in yellow and nearby residues are in grey sticks, protein backbone is in colour ribbons, H-bond and π - π interactions are shown as dashed lines. (For interpretation of the references to colour in this figure legend, the reader is referred to the web version of this article.)

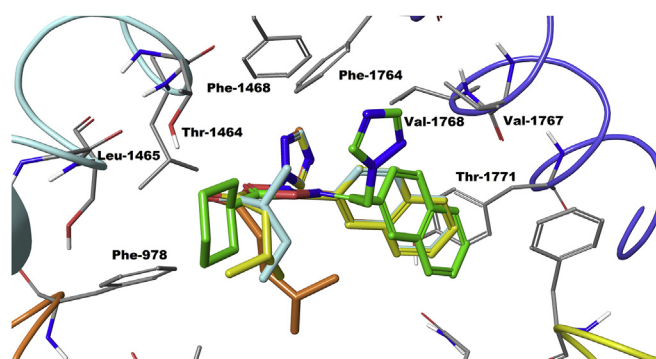


Fig. 5. Superimposition of the docking conformations of **5e** (turquoise), **5f** (yellow), **5j** (orange), and **5l** (green) in the active site of Na^+ channel inner pore (top view). Ligands are in colour, nearby residues are in grey sticks, protein backbone in colour ribbons. (For interpretation of the references to colour in this figure legend, the reader is referred to the web version of this article.)

Table 6
Docking scores of **5e**, **5f**, **5j**, and **5l**.

Comp.	Docking score		Ligand efficiency		H-bond score		Internal energy		VDW energy		Coulomb energy	
	VGSC	GABA _A R	VGSC	GABA _A R	VGSC	GABA _A R	VGSC	GABA _A R	VGSC	GABA _A R	VGSC	GABA _A R
5e	-4.66	-6.37	-0.19	-0.26	-0.70	-0.70	6.98	1.61	-30.36	-24.05	-3.33	-3.72
5f	-4.71	-6.70	-0.19	-0.27	-0.70	-0.57	2.41	1.10	-29.78	-29.20	-3.82	-4.62
5j	-4.24	-6.69	-0.18	-0.26	-0.70	-0.55	9.29	3.05	-30.99	-29.86	-3.67	-4.86
5l	-3.42	-6.32	-0.13	-0.23	-0.20	0.00	1.31	6.97	-29.88	-29.39	-0.17	-0.91

affinity. The inactive derivative **5a**, assuming a flipped conformation, failed to π -stack with Phe-1468 aromatic side chain as the triazole ring positioned towards inner pore instead (see [Figure S.1A](#) of Supplementary Data).

Docking scores and other scoring terms are summarized in [Table 6](#). The docking scores of the four compounds were pretty close to each other. **5e** and **5j** had relatively high internal energy, indicative of high strain on their docked conformations in Na⁺ channel inner pore. As **5l** did not have H-bond with Thr-1464 and π - π stacking with Phe-1468 either, its H-bond score and Coulomb energy was higher.

According to the per-residue interactions scores DIII- and DIV-S6 residues were responsible for most of the interactions with **5f**. Phe-1764, Thr-1771, and Leu-1465 were among those residues with the lowest interaction scores. Apart from these residues Thr-1464 and Phe-1468 of DIII-S6 and Val-1768 and Val-1767 of DIV-S6 were important contributors of ligand-receptor complex, however the corresponding residues of Val-1768 and Thr-1464 in Na_v1.4, namely Val-1583 and Thr-1279, respectively, were showed by alanine substitution to have no effect on binding affinities of LAs [31].

2.3.2. GABA_AR docking

We docked our compounds into the putative GABA and benzodiazepine (BZD) binding sites between extracellular domains (ECD) of β_2 and α_1 and α_1 and γ_2 subunits, respectively. These sites include loop A-F, where most of the residues that affect ligand binding and constitute part of binding sites are present [38]. No docking pose was obtained for the GABA binding site, thus we suggest that our compounds are too bulky for this site and unlikely to be GABA_AR agonists.

On the other hand the compounds fit well into the BZD binding site ([Fig. 6](#)). The triazole ring of **5f** and the ethylene chain attached to it corresponded to the fused ring system (so called L1 pharmacophore) of diazepam present in the model. The triazole ring engaged in vertical π - π stacking with γ_2 Phe-77 and close contacts

with α_1 His-101 and γ_2 Tyr-58. This ring also formed a hydrogen bond via its N₂ with α_1 Ser-204. Among these residues α_1 His-101 and γ_2 Phe-77 are necessary for high-affinity binding of ligands to this site, according to the site directed mutagenesis studies [39–44]. The naphthalene ring of **5f** situated in the hydrophobic cleft surrounded by the aromatic side chains of γ_2 Phe-77, α_1 Phe-99, and α_1 Tyr-159, exactly where the phenyl ring of diazepam (L3) lied in the model, making π - π stacking with them. This ring also interacted with γ_2 Asn-128 and γ_2 Arg-144. α_1 Phe-99 and α_1 Tyr-159 were previously reported to be involved in BZD-like ligand binding and part of the binding site [45,46]. Positioned in the gap between two subunits and close to loop C, the isobutanoyl moiety of **5f** was in close contacts with α_1 Thr-206, γ_2 Leu-140, and γ_2 Thr-142. This gap is not deep enough for larger moieties like those of **5m** and **5n** to fit and this may account for their lack of activity. Mutations on α_1 Thr-206 reportedly decreased binding affinity of ligands to this site significantly [44,47–50]. Diazepam, instead, reportedly engaged in two hydrogen bonds with α_1 Thr-206 and γ_2 Thr-142 as to build a bridge between two subunits [15]. The interactions of *N*-methyl group of diazepam was not satisfied by our compounds.

Almost the same interactions were observed for **5e**, **5j**, and **5l** except that **5l** did not form H-bond with α_1 Ser-204 and π - π stacking with γ_2 Phe-77 either ([Fig. 7](#)). Their docking scores were quite close to each other and indicated strong binding to the BZD binding site ([Table 5](#)). **5a**, however, failed to interact Phe-99, which could account for its inefficacy (see [Fig. S.1B](#) of Supplementary Data). The internal energy of **5l** was relatively high and its electrostatic interactions were low, showing that the conformation this compound assumed to fit in the narrow gap between α_1 and γ_2 subunits caused high strain. According to the per-residue interactions scores of **5f** γ_2 Phe-77, α_1 Ser-204, γ_2 Tyr-58, γ_2 Thr-142, α_1 His-101, and γ_2 Asn-128 were the highest-contributing residues to GABA_AR binding. The docking poses mainly complied with the experimental and theoretical data regarding the interactions of GABA_AR positive allosteric modulators with the BZD binding site residues. Therefore, our compounds could activate GABA_ARs in a similar way the BZD-like compounds do and this activation could

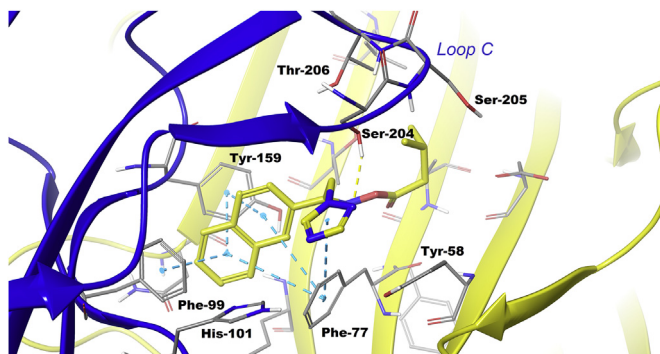


Fig. 6. Docking conformation of **5f** in the BZD-binding site of GABA_AR. **5f** is in yellow and nearby residues are in grey sticks, protein backbone is in colour ribbons, H-bond and π - π interactions are shown as dashed lines. (For interpretation of the references to colour in this figure legend, the reader is referred to the web version of this article.)

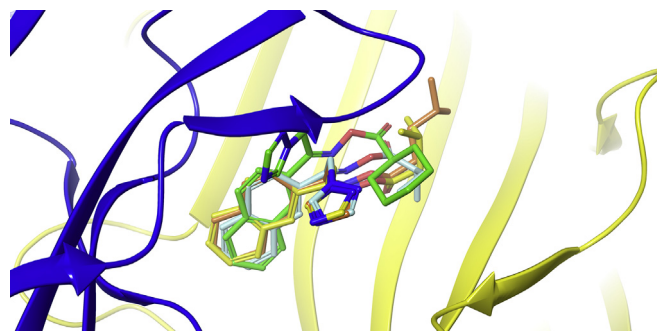


Fig. 7. Superimposition of docking conformations of **5e** (turquoise), **5f** (yellow), **5j** (orange), and **5l** (green) in the BZD-binding site of GABA_AR. Ligands are in colour sticks, protein backbone in colour ribbons. (For interpretation of the references to colour in this figure legend, the reader is referred to the web version of this article.)

partly or wholly account for their efficacy.

3. Conclusion

Aiming to find safe, selective, and more efficacious novel AEDs, we prepared 14 new oxime ester derivatives and screened them *in vivo* for their anticonvulsant and neurotoxic effects. Among them 10 compounds showed protection against MES- and/or s.c. MET-induced seizures without causing neurotoxicity. One of them (**5f**) was active at 30 mg/kg in s.c. MET test at 4 h. 1-(2-Naphthyl)-2-(1H-1,2,4-triazol-1-yl)ethanone oxime (**4**) was previously found inactive in the same animal models of seizure [24] which makes it less likely that our active compounds act as prodrugs. Two of the inactive derivatives, **5m** and **5n**, were predicted nondrug-like according to some of the algorithms calculated by MLViS web tool, which shows the importance of drug-likeness prediction for anticonvulsant activity. However it was not possible to establish SARs for these compounds regarding anticonvulsant activity and neurotoxicity. Relatively high *clogP* values, indicative of high lipophilicity, could be one of the reasons for the absence of anticonvulsant activity at lower doses.

VGSC inhibition and positive allosteric modulation of GABA_AR are possible anticonvulsant mechanisms of action for our active compounds therefore we performed molecular docking studies of **5e**, **5f**, **5j**, and **5l** using homology models of Na⁺ channel inner pore and GABA_AR. The docking solutions obtained in VGSC active site were in accordance with those previously found for phenytoin, carbamazepine, and lamotrigine and with the experimental findings thereof [14,31–34]. Phe-1764, Tyr-1771, and Leu-1465 were among the residues with the highest affinity according to the per-residue interaction scores from Glide. On the other hand docking poses obtained in the BZD binding site of GABA_AR were somewhat similar to the diazepam binding model [15] and mostly in accordance with the mutagenesis data [39–50]. However, docking results of **5a**, one of the inactive derivatives, showed that this compound failed certain key interactions with both receptors. We suggest that our compounds might inhibit VGSCs by sterically occluding the channel inner pore and are stabilized mainly by the key hydrophobic and electrostatic interactions with DIV- and DIII-S6 residues in a similar manner suggested for phenytoin, carbamazepine, and lamotrigine [14]. They might as well modulate GABA_ARs by binding with high affinity to the BZD binding site but not to the orthosteric binding site. We found that these interactions together were only possible for the *Z* isomers, which supports our hypothesis considering the X-ray crystallographic data obtained for **4**. Docking studies also revealed that increasing the size of the “R” group would probably hinder binding of our compounds to the putative binding sites, which could underlie the inefficacy of **5m** and **5n**.

4. Experimental part

4.1. Chemistry

All the chemicals used in this study were purchased from E. Merck, Fluka AG, and Aldrich. Milestone SartsYNTH (USA) microwave reactor was used for microwave-assisted synthesis. Merck Kieselgel 60 F₂₅₄ plates were used for thin layer chromatography. Melting points were determined using a Barnstead Electrothermal 9100 (USA) capillary melting point apparatus and uncorrected. The column chromatography was performed using Kieselgel 60 (0.040–0.063 mm) (230–400 mesh ASTM) silica gel (Merck, Germany). IR spectra were recorded with a Perkin Elmer Spectrum One FTIR spectrometer using Attenuated Total Reflectance apparatus. ¹H NMR spectra of the compounds were recorded with Bruker Avance

300 MHz Ultrashield™ (Germany) NMR spectrometer and mass spectra with Micromass ZQ (USA) using electro spray ionization (ESI+) method and MassLynx 4.1 software. All chemical shifts are reported as δ (ppm) values. Splitting patterns are designated as follows: s: singlet; d: doublet; t: triplet; q: quartet; and m: multiplet. Elemental analyses were performed using an LECO 932 CHNS elemental analysis apparatus (USA).

4.1.1. Synthesis of the compounds

4.1.1.1. Preparation of 2-bromo-1-(2-naphthyl)ethanone (**2**), 1-(2-naphthyl)-2-(1H-1,2,4-triazol-1-yl)ethanone (**3**), and 1-(2-naphthyl)-2-(1H-1,2,4-triazol-1-yl)ethanone oxime (**4**). 2-Bromo-1-(2-naphthyl)ethanone (**2**), 1-(2-naphthyl)-2-(1H-1,2,4-triazol-1-yl)ethanone (**3**), and 1-(2-naphthyl)-2-(1H-1,2,4-triazol-1-yl)ethanone oxime (**4**) were prepared according to the methods elucidated in the relative literature [16–18]. MW irradiation was applied during synthesis of **3** and **4** instead of refluxing. The reaction media were kept at room temperature for 3 min then heated up to 70 °C and irradiated for 8 min under maximum power of 500 W. Completion of the reactions was determined via thin-layer chromatography.

4.1.1.2. Oxime esters (**5a–n**). **5a–c**, **5e–n**: A mixture of DCC (2 mmol) and DMAP (0.17 mmol) in dry DCM was added dropwise to a mixture of 1-(2-naphthyl)-2-(1H-1,2,4-triazol-1-yl)ethanone oxime (1 mmol) and proper carboxylic acid (2 mmol) in dry DCM at 0–5 °C. The resulting mixture was stirred for 0.5 h at 0–5 °C and for an additional 3–6 h at room temperature. The precipitate was filtered off, the filtrate was evaporated to dryness, and the resulting residue was purified via column chromatography. HCl salts of the compounds were obtained by addition of ethereal solution of HCl to their ethereal solution and crystallized from proper solvents. **5c**, **5e**, **5l**, and **5n** were not converted to their HCl salts.

5d: The mixture of 1-(2-naphthyl)-2-(1H-1,2,4-triazol-1-yl)ethanone (1 mmol), DMAP (0.17 mmol), and butyric anhydride (2 mmol) in dry DCM was stirred at room temperature for 6 h. The precipitate which occurred with addition of diethyl ether was filtered off and the filtrate was evaporated till dryness. The resulting residue was purified via column chromatography.

4.1.1.2.1. 1-(2-Naphthyl)-2-(1H-1,2,4-triazol-1-yl)ethanone *O*-propanoyloxime hydrochloride (**5a**). IR (ν cm⁻¹) 3142, 3009 (aromatic C–H), 2983 (aliphatic C–H), 1769 (C=O), 1599 (C=N). ¹H NMR (CDCl₃, 300 MHz) δ 1.06 (39%), 1.21 (61%) (t, *J* = 7.5 Hz, 3H, CH₃), 2.21–2.32 (39%), 2.52–2.60 (61%) (q, 2H, CH₂CO), 5.61 (37%), 5.70 (63%) (s, 2H, CH₂N), 7.44–8.17 (m, 7H, naphthalene), 8.15 (37%), 8.26 (63%) (s, 1H, H³, triazole), 8.78 (37%), 9.12 (63%) (s, 1H, H⁵, triazole). ESI+: *m/e* 332 ([M+Na+H]⁺), 331 ([M+Na]⁺), 309 ([M+H]⁺), 235 (100%). Anal. Calcd. for C₁₇H₁₇ClN₄O₂·1/3H₂O (350.81): C, 58.21; H, 5.08; N, 15.97; Found: C, 58.10; H, 5.06; N, 16.37%.

4.1.1.2.2. 1-(2-Naphthyl)-2-(1H-1,2,4-triazol-1-yl)ethanone *O*-(2-methyl)propanoyloxime hydrochloride (**5b**). IR (ν cm⁻¹) 3136, 3045 (aromatic C–H), 2975 (aliphatic C–H), 1722 (C=O), 1561 (C=N). ¹H NMR (CDCl₃-d, 300 MHz) δ 1.06 (49%), 1.09 (51%) (d, *J* = 7 Hz, 6H, CH₃), 2.37–2.50 (49%), 2.69–2.78 (51%) (m, 1H, CHCO), 5.56 (49%), 5.67 (51%) (s, 2H, CH₂N), 6.65–8.08 (m, 7H, naphthalene), 8.12 (49%), 8.22 (51%) (s, 1H, H³, triazole), 8.54 (49%), 8.90 (51%) (s, 1H, H⁵, triazole). ESI+: *m/e* 323 ([M+H]⁺), 235, 123 (100%). Anal. Calcd. for C₁₈H₁₉ClN₄O₂·1/3H₂O (364.83): C, 59.26; H, 5.43; N, 15.36; Found: C, 58.79; H, 5.33; N, 15.82%.

4.1.1.2.3. 1-(2-Naphthyl)-2-(1H-1,2,4-triazol-1-yl)ethanone *O*-trimethylacetyloxime (**5c**). IR (ν cm⁻¹) 3116 (aromatic C–H), 2975 (aliphatic C–H), 1755 (C=O), 1500 (C=N). ¹H NMR (CDCl₃-d, 300 MHz) δ 1.35 (s, 9H, CH₃), 5.65 (s, 2H, CH₂N), 7.53–7.96 (m, 7H, naphthalene), 8.13 (s, 1H, H³, triazole), 8.25 (s, 1H, H⁵, triazole).

ESI+: m/e 359 ([M+Na]⁺, 100%), 322, 235. Anal. Calcd. for C₁₉H₂₀N₄O₂·1/4H₂O (340.90): C, 66.94; H, 6.06; N, 16.44; Found: C, 67.45; H, 6.15; N, 16.24%.

4.1.1.2.4. 1-(2-Naphthyl)-2-(1H-1,2,4-triazol-1-yl)ethanone O-butanoyloxime (**5d**). IR (ν cm⁻¹) 3108 (aromatic C–H), 2968 (aliphatic C–H), 1769 (C=O), 1506 (C=N). ¹H NMR (CDCl₃-d, 300 MHz) δ 0.91 (5%), 1.06 (95%) (t, J = 7.5 Hz, 3H, CH₃), 1.60–1.66 (5%), 1.77–1.84 (95%) (m, 2H, CH₂CH₃), 2.30 (5%), 2.57 (95%) (t, J = 7.5 Hz, 2H, CH₂CO), 5.50 (5%), 5.65 (95%) (s, 2H, CH₂N), 7.52–7.98 (m, 6H, H^{3–8}, naphthalene), 7.95 (s, 1H, H³, triazole), 8.20 (s, 1H, H⁵, triazole), 8.31 (m, 1H, H¹, naphthalene). ESI+: m/e 345 ([M+Na]⁺), 323 ([M+H]⁺), 235 (100%). Anal. Calcd. for C₁₈H₁₈N₄O₂·1/2H₂O (331.37): C, 65.24; H, 5.78; N, 16.91; Found: C, 64.95; H, 5.50; N, 16.98%.

4.1.1.2.5. 1-(2-Naphthyl)-2-(1H-1,2,4-triazol-1-yl)ethanone O-(2-methyl)butanoyloxime (**5e**). IR (ν cm⁻¹) 3115 (aromatic C–H), 2971, 235 (aliphatic C–H), 1751 (C=O), 1502 (C=N). ¹H NMR (CDCl₃-d, 300 MHz) δ 1.00 (t, J = 7.5 Hz, 3H, CH₂CH₃), 1.30 (d, J = 7.2 Hz, 3H, CHCH₃), 1.59–1.69 (m, 1H, H^a, CHCH₂), 1.75–1.91 (m, 1H, H^b, CHCH₂), 2.58 (m, 1H, CH), 5.65 (s, 2H, CH₂N), 7.51–7.98 (m, 7H, naphthalene), 8.17 (s, 1H, H³, triazole), 8.30 (s, 1H, H⁵, triazole). ESI+: m/e 360 ([M+Na+H]⁺, 100%), 359 ([M+Na]⁺), 235. Anal. Calcd. for C₁₉H₂₀N₄O₂ (336.40): C, 67.84; H, 5.99; N, 16.66; Found: C, 67.65; H, 5.85; N, 16.44%.

4.1.1.2.6. 1-(2-Naphthyl)-2-(1H-1,2,4-triazol-1-yl)ethanone O-(3-methyl)butanoyloxime hydrochloride (**5f**). IR: ν (cm⁻¹) 3116, 3006 (aromatic C–H), 2969 (aliphatic C–H), 1759 (C=O), 1562 (C=N). ¹H NMR (CDCl₃-d, 300 MHz) δ 0.92 (31%), 1.07 (69%) (d, J = 6.6 Hz, 6H, CH₃), 2.02–2.13 (31%), 2.16–2.31 (69%) (m, 1H, CH), 2.18 (31%), 2.47 (69%) (d, J = 6.9 Hz, 2H, CH₂CO), 5.81 (31%), 5.90 (69%) (s, 2H, CH₂N), 6.74–8.24 (m, 7H, naphthalene), 8.03 (31%), 8.38 (69%) (s, 1H, H³, triazole), 9.60 (31%), 9.77 (69%) (s, 1H, H⁵, triazole). ESI+: m/e 359 ([M+Na]⁺), 337 ([M+H]⁺), 123 (100%). Anal. Calcd. for C₁₉H₂₁ClN₄O₂·1/2H₂O (381.15): C, 59.76; H, 5.81; N, 14.67; Found: C, 60.18; H, 5.63; N, 14.79%.

4.1.1.2.7. 1-(2-Naphthyl)-2-(1H-1,2,4-triazol-1-yl)ethanone O-pentanoyloxime hydrochloride (**5g**). IR (ν cm⁻¹) 3124, 3009 (aromatic C–H), 2959 (aliphatic C–H), 1762 (C=O), 1601 (C=N). ¹H NMR (CDCl₃-d, 300 MHz) δ 0.84 (30%), 0.97 (69%) (t, J = 7.3 Hz, 3H, CH₃), 1.23–1.38 (31%), 1.40–1.48 (69%) (m, 2H, CH₂CH₃), 1.50–1.60 (31%), 1.65–1.79 (70%) (m, 2H, CH₂CH₂CH₃), 2.31 (34%), 2.61 (66%) (t, J = 7.5 Hz, 2H, CH₂CO), 5.78 (30%), 5.86 (70%) (s, 2H, CH₂N), 7.32–8.15 (m, 7H, naphthalene), 8.17 (30%), 8.36 (70%) (s, 1H, H³, triazole), 9.49 (30%), 9.69 (70%) (s, 1H, H⁵, triazole). ESI+: m/e 359 ([M+Na]⁺), 337 (M+H), 235 (100%). Anal. Calcd. for C₁₉H₂₁ClN₄O₂·1/5H₂O (376.45): C, 60.62; H, 5.73; N, 14.88; Found: C, 60.34; H, 5.49; N, 15.52%.

4.1.1.2.8. 1-(2-Naphthyl)-2-(1H-1,2,4-triazol-1-yl)ethanone O-(2-methyl)pentanoyloxime hydrochloride (**5h**). IR (ν cm⁻¹) 3119, 3009 (aromatic C–H), 2958 (aliphatic C–H), 1758 (C=O), 1538 (C=N). ¹H NMR (CDCl₃-d, 300 MHz) δ 0.80 (35%), 0.96 (65%) (t, J = 7.2 Hz, 3H, CH₂CH₃), 1.11 (38%), 1.30 (62%) (d, J = 7 Hz, 3H, CHCH₃), 1.16–1.26 (29%), 1.33–1.45 (71%) (m, 2H, CH₂CH₃), 1.47–1.61 (37%), 1.65–1.84 (63%) (m, 2H, CH₂CH), 2.37–2.49 (35%), 2.71–2.81 (65%) (m, 1H, CH), 5.80 (35%), 5.88 (65%) (s, 2H, CH₂N), 7.28–8.19 (m, 7H, naphthalene), 8.02 (35%), 8.37 (65%) (s, 1H, H³, triazole), 9.58 (35%), 9.86 (65%) (s, 1H, H⁵, triazole). ESI+: m/e 373 ([M+Na]⁺), 351 ([M+H]⁺), 235 (100%). Anal. Calcd. for C₂₀H₂₃ClN₄O₂ (386.88): C, 62.09; H, 5.99; N, 14.48; Found: C, 62.41; H, 5.59; N, 14.45%.

4.1.1.2.9. 1-(2-Naphthyl)-2-(1H-1,2,4-triazol-1-yl)ethanone O-(3-methyl)pentanoyloxime hydrochloride (**5i**). IR (ν cm⁻¹) 3117, 3008 (aromatic C–H), 2964 (aliphatic C–H), 1758 (C=O), 1562 (C=N). ¹H NMR (CDCl₃-d, 300 MHz) δ 0.80 (35%), 0.93 (65%) (t, J = 7.4 Hz, 3H, CH₃), 0.78 (35%), 1.02 (65%) (d, J = 6.7 Hz, 3H, CHCH₃), 1.13–1.51 (m, 2H, CH₂CH₃), 1.77–2.04 (m, 1H, CH), 2.05–2.64 (m, 2H, CH₂CO), 5.91

(35%), 6.00 (65%) (s, 2H, CH₂N), 7.28–8.40 (m, 8H, H³, triazole, naphthalene), 10.36 (35%), 10.43 (65%) (s, 1H, H⁵, triazole). ESI+: m/e 373 ([M+Na]⁺), 351 ([M+H]⁺), 123 (100%). Anal. Calcd. for C₂₀H₂₃ClN₄O₂·H₂O (404.89): C, 59.33; H, 6.22; N, 13.84; Found: C, 59.91; H, 5.93; N, 14.16%.

4.1.1.2.10. 1-(2-Naphthyl)-2-(1H-1,2,4-triazol-1-yl)ethanone O-(4-methyl)pentanoyloxime hydrochloride (**5j**). IR (ν cm⁻¹) 3133, 3009 (aromatic C–H), 2954 (aliphatic C–H), 1765 (C=O), 1561 (C=N). ¹H NMR (CDCl₃-d, 300 MHz) δ 0.82 (34%), 0.95 (66%) (d, J = 6.2 Hz, 6H, CH₃), 0.90–0.92 (m, 1H, CH), 1.45–1.53 (39%), 1.58–1.69 (61%) (m, 2H, CH₂CH), 2.30 (39%), 2.61 (61%) (t, J = 7.5 Hz, 2H, CH₂CO), 5.83 (33%), 5.92 (67%) (s, 2H, CH₂N), 7.50–8.24 (m, 7H, naphthalene), 8.05 (33%), 8.38 (67%) (1H, s, H³, triazole), 9.83 (32%), 10.00 (68%) (s, 1H, H⁵, triazole). ESI+: m/e 373 ([M+Na]⁺), 351 ([M+H]⁺), 123 (100%). Anal. Calcd. for C₂₀H₂₃ClN₄O₂·1/2H₂O (395.89): C, 60.68; H, 6.11; N, 14.15; Found: C, 61.03; H, 5.84; N, 14.56%.

4.1.1.2.11. 1-(2-Naphthyl)-2-(1H-1,2,4-triazol-1-yl)ethanone O-(3-propyl)pentanoyloxime hydrochloride (**5k**). IR (ν cm⁻¹) 3116, 3009 (aromatic C–H), 2959 (aliphatic C–H), 1757 (C=O), 1541 (C=N). ¹H NMR (CDCl₃-d, 300 MHz) δ 0.80 (43%), 0.95 (57%) (t, J = 7.4 Hz, 6H, CH₃), 1.16–1.82 (m, 8H, 2CH₂CH₂), 2.30–2.37 (42%), 2.63–2.71 (58%) (m, 1H, CH), 5.90 (44%), 6.01 (56%) (s, 2H, CH₂N), 7.50–8.43 (m, 9H, naphthalene, triazole). ESI+: m/e 401 ([M+Na]⁺), 379 ([M+H]⁺), 123 (100%). Anal. Calcd. for C₂₂H₂₇ClN₄O₂ (414.93): C, 63.40; H, 6.51; N, 13.45; Found: C, 63.40; H, 6.51; N, 13.45%.

4.1.1.2.12. 1-(2-Naphthyl)-2-(1H-1,2,4-triazol-1-yl)ethanone O-cyclohexylcarbonyloxime (**5l**). IR (ν cm⁻¹) 3120 (aromatic C–H), 2932 (aliphatic C–H) 1748 (C=O), 1500 (C=N). ¹H NMR (CDCl₃-d, 300 MHz) δ 1.13–2.00 (m, 10H, 5CH₂, cyclohexane), 2.53–2.63 (m, 1H, CH, cyclohexane), 5.65 (s, 2H, CH₂N), 7.51–7.97 (m, 7H, naphthalene), 8.17 (s, 1H, H³, triazole), 8.29 (s, 1H, H⁵, triazole). ESI+: m/e 385 ([M+Na]⁺, 100%), 236, 235. Anal. Calcd. for C₂₁H₂₂N₄O₂·1/3H₂O (368.44): C, 68.46; H, 6.20; N, 15.21; Found: C, 69.02; H, 6.34; N, 14.73%.

4.1.1.2.13. 1-(2-Naphthyl)-2-(1H-1,2,4-triazol-1-yl)ethanone O-phenylacetylloxime hydrochloride (**5m**). IR (ν cm⁻¹) 3133 (aromatic C–H), 2958 (aliphatic C–H), 1774 (C=O), 1536 (C=N). ¹H NMR (CDCl₃-d, 300 MHz) δ 3.51 (s, 2H, CH₂CO), 5.53 (s, 2H, CH₂N), 6.65–9.01 (m, 14H, benzene, naphthalene, triazole). ESI+: m/e 393 ([M+Na]⁺), 371 ([M+H]⁺), 123 (100%). Anal. Calcd. for C₂₂H₁₉ClN₄O₂·H₂O (424.88): C, 62.19; H, 4.98; N, 13.19; Found: C, 61.91; H, 4.97; N, 13.40%.

4.1.1.2.14. 1-(2-Naphthyl)-2-(1H-1,2,4-triazol-1-yl)ethanone O-(E)-3-phenylprop-2-enoyloxime (**5n**). IR (ν cm⁻¹) 3104 (aromatic C–H), 1746 (C=O), 1633 (alkenyl C=C), 1505 (C=N). ¹H NMR (CDCl₃-d, 300 MHz) δ 5.73 (s, 2H, CH₂N), 6.64 (d, J = 15.9 Hz, 1H, COCH), 7.41–8.02 (m, 12H, benzene, naphthalene, CH-Ph), 8.25 (s, 1H, H³, triazole), 8.33 (s, 1H, H⁵, triazole). ESI+: m/e 405 ([M+Na]⁺, 100%), 236, 235. Anal. Calcd. for C₂₃H₁₈N₄O₂·1/3H₂O (388.43): C, 71.12; H, 4.84; N, 14.4; Found: C, 71.41; H, 4.62; N, 14.4%.

4.2. Pharmacology

Male Swiss albino mice of 25±2 g weight provided by the Institution of Veterinary Control and Research Institute, Elazig, Turkey, and Dual Impedance Research Stimulator (Harvard), corneal electrodes, PEG 400 (Merck), and rotarod were used for the anticonvulsant and neurotoxicity evaluation of the compounds. Screenings were fulfilled in the laboratories of Laboratory Animal Production Centre of Inonu University and Hacettepe University Faculty of Pharmacy Department of Pharmaceutical Chemistry laboratories according to the protocol of National Institute of Neurological Disorder and Stroke (NINDS) Epilepsy Therapy

Screening Program (ETSP) (formerly known as Anticonvulsant Screening Program) [51] with the permission granted by the Laboratory Animals Ethic Committee of Inonu University, Malatya, Turkey (permission date and number: 29.11.2011, 2011/A92).

Suspensions of each compound in PEG 400 at 30, 100, and 300 mg/kg concentrations were intraperitoneally administered to the mice 0.5 or 4 h prior to seizure induction. In MES test the mice were applied 0.9% saline in the corneas and electrocuted for 0.2 s with 60 Hz alternative current using a pair of electrodes and the mice with a hind limb tonic extension of less than 90° were considered to be protected by the administered compound. In s.c. MET test 85 mg/kg of metrazol was injected subcutaneous in the midline of the neck to induce seizure then the mice were observed for the next 30 min. The mice without an episode of clonic spasms, approximately 3–5 s, of the fore and/or hind limbs, jaws, or vibrissae were considered to be protected by the administered compound. A negative control was performed by evaluation of the responses from placebo (PEG)-administered mice to seizure induction and mice were observed to undergo the episodes specific for each model [51].

Prior to seizure induction the mice were put on a rod revolving at 6 rpm. Those which fell off the rod three times in 1 min were considered toxic and the compounds administered to them were deemed to have neurotoxicity. Placebo-administered mice were observed to succeed the test [51].

4.3. Molecular docking studies

Ligands were sketched on MarvinSketch and their physico-chemical properties were calculated using Calculator Plugins, Marvin 15.5.25.0, 2015, ChemAxon (<http://www.chemaxon.com>). Ligands were prepared for docking using LigPrep, version 3.6, Schrödinger, LLC, New York, NY, 2015. OPLS 2005 force field parameters were used for their minimization [52]. The open/activated Na⁺ channel inner pore and GABA_AR structure models were obtained from the related literature [14,15]. The coordinates of the docked ligands (phenytoin for VGSC, GABA and diazepam for GABA_AR) were set as centres of search space for grid generation and docking. Following settings were used on Glide, version 6.9, Schrödinger, LLC, New York, NY, 2015: Extra precision was set, ligands were kept flexible, 10 poses were written at most per ligand, post-minimization was enabled and per-residue interaction scores for residues within 12 Å of grid centre were written. Maestro, version 10.4, Schrödinger, LLC, New York, NY, 2015, was used as the user interface during all procedures. Phenytoin and diazepam were re-docked into their binding sites and their original conformations were reproduced (RMSD: 1.28 Å for phenytoin and 0.84 Å for diazepam). Docking solutions were visually inspected using pose viewer of Maestro.

4.4. X-ray crystallography

Single crystal data was collected with RIGAKU R-Axis Rapid II DW with Dual Wavelength Micro Max 007DW XG and VariMax DW optics single crystal X-ray diffractometer system with curved imaging plate detector. The data collection, cell refinement and data reduction were performed by CrystalClear-SM Expert 2.0 r16 [53] program. The crystal structure was solved by using SIR-2011 [54] and refined by using the SHELXL [55].

Conflict of interest

Authors declare no conflict of interest.

Acknowledgements

We are thankful to Prof. Dr. Erhan Palaska for providing mass spectra of some of the compounds.

Appendix A. Supplementary data

Supplementary data associated with this article can be found in the online version, at <http://dx.doi.org/10.1016/j.ejmech.2016.08.032>. These data include MOL files and InChIKeys of the most important compounds described in this article.

References

- [1] M.J. England, C.T. Liverman, A.M. Schultz, L.M. Strawbridge, Epilepsy across the spectrum: promoting health and understanding, *Epilepsy Behav.* 25 (2012) 266–276.
- [2] R.A. Scott, S.D. Lhatoo, J.W. Sander, The treatment of epilepsy in developing countries: where do we go from here? *B. World Health Organ.* 79 (2001) 344–351.
- [3] D. Schmidt, Drug treatment of epilepsy: options and limitations, *Epilepsy Behav.* 15 (2009) 56–65.
- [4] D. Nardì, A. Tajana, A. Leonardi, R. Pennini, F. Portioli, M.J. Magistretti, A. Subissi, Synthesis and anticonvulsant activity of N-(benzoylalkyl) imidazoles and N-(omega-phenyl-omega-hydroxyalkyl) imidazoles, *J. Med. Chem.* 24 (1981) 727–731.
- [5] K.A. Walker, M.B. Wallach, D.R. Hirschfeld, 1-(Naphthylalkyl)-1H-imidazole derivatives, a new class of anticonvulsant agents, *J. Med. Chem.* 24 (1981) 67–74.
- [6] P. Granger, B. Biton, C. Faure, X. Vige, H. Depoortere, D. Graham, S.Z. Langer, B. Scatton, P. Avenet, Modulation of the gamma-aminobutyric acid type A receptor by the antiepileptic drugs carbamazepine and phenytoin, *Mol. Pharmacol.* 47 (1995) 1189–1196.
- [7] R.L. Macdonald, K.M. Kelly, Antiepileptic drug mechanisms of action, *Epilepsia* 36 (1995) S2–S12.
- [8] D.W. Robertson, J.H. Krushinski, E. Beedle, J.D. Leander, D.T. Wong, R. Rathbun, Structure-activity relationships of (arylalkyl) imidazole anticonvulsants: comparison of the (fluorenylalkyl) imidazoles with nafimidone and denzimol, *J. Med. Chem.* 29 (1986) 1577–1586.
- [9] S. Dalkara, A. Karakurt, Recent progress in anticonvulsant drug research: strategies for anticonvulsant drug development and applications of antiepileptic drugs for non-epileptic central nervous system disorders, *Curr. Top. Med. Chem.* 12 (2012) 1033–1071.
- [10] A. Karakurt, M.D. Aytimir, J.P. Stables, M. Özalp, F. Betül Kaynak, S. Özbey, S. Dalkara, Synthesis of some oxime ether derivatives of 1-(2-naphthyl)-2-(1, 2, 4-triazol-1-yl)ethanone and their anticonvulsant and antimicrobial activities, *Arch. Pharm.* 339 (2006) 513–520.
- [11] A. Karakurt, M. Özalp, Ş. Işık, J.P. Stables, S. Dalkara, Synthesis, anticonvulsant and antimicrobial activities of some new 2-acetylnaphthalene derivatives, *Bioorg. Med. Chem.* 18 (2010) 2902–2911.
- [12] A. Karakurt, M.A. Alagöz, B. Sayoğlu, Ü. Çalış, S. Dalkara, Synthesis of some novel 1-(2-naphthyl)-2-(imidazol-1-yl)ethanone oxime ester derivatives and evaluation of their anticonvulsant activity, *Eur. J. Med. Chem.* 57 (2012) 275–282.
- [13] C.O. Kappe, Controlled microwave heating in modern organic synthesis, *Angew. Chem. Int. Ed.* 43 (2004) 6250–6284.
- [14] G.M. Lipkind, H.A. Fozzard, Molecular model of anticonvulsant drug binding to the voltage-gated sodium channel inner pore, *Mol. Pharmacol.* 78 (2010) 631–638.
- [15] R. Bergmann, K. Kongsbak, P.L. Sørensen, T. Sander, T. Balle, A Unified model of the GABA_A receptor comprising agonist and benzodiazepine binding sites, *PLoS One* 8 (2013) e52323.
- [16] T. Immediata, A.R. Day, β-Naphthyl derivatives of ethanalamine and n-substituted ethanalamines, *J. Org. Chem.* 5 (1940) 512–527.
- [17] Ü. Çalış, S. Dalkara, M. Ertan, R. Sunal, The significance of the imidazole ring in anticonvulsant activity of (arylalkyl) imidazoles, *Arch. Pharm.* 321 (1988) 841–846.
- [18] H. Baji, M. Flammang, T. Kimny, F. Gasquez, P. Compagnon, A. Delcourt, Synthesis and antifungal activity of novel (1-aryl-2-heterocyclyl)ethylideneaminoxymethyl-substituted dioxolanes, *Eur. J. Med. Chem.* 30 (1995) 617–626.
- [19] B. Neises, W. Steglich, Simple method for the esterification of carboxylic acids, *Angew. Chem. Int. Ed.* 17 (1978) 522–524.
- [20] A.L. Spek, Structure validation in chemical crystallography, *Acta Crystallogr. Sect. D.* 65 (2009) 148–155.
- [21] L.J. Farrugia, ORTEP-3 for windows – a version of ORTEP-III with a graphical user interface (GUI), *J. Appl. Crystallogr.* 30 (1997) 565.
- [22] A. Balsamo, B. Macchia, A. Martinelli, E. Orlandini, A. Rossello, F. Macchia, G. Broccoli, P. Domiano, Synthesis and antimicrobial properties of substituted 3-aminoxy-(E)-2-methoxyiminopropionyl penicillins and cephalosporins, *Eur.*

- J. Med. Chem. 25 (1990) 227–233.
- [23] R.J. Stoodley, Molecular rearrangements, in: B. Capon, C.W. Rees (Eds.), *Organic Reaction Mechanisms*, John Wiley & Sons Ltd., London, 1972, pp. 265–267.
- [24] A. Karakurt, S. Dalkara, M. Özalp, S. Özbey, E. Kendi, J.P. Stables, Synthesis of some 1-(2-naphthyl)-2-(imidazole-1-yl) ethanone oxime and oxime ether derivatives and their anticonvulsant and antimicrobial activities, *Eur. J. Med. Chem.* 36 (2001) 421–433.
- [25] S. Korkmaz, G. Zararsiz, D. Goksuluk, MLViS: a Web tool for machine learning-based virtual screening in early-phase of drug discovery and development, *PLoS One* 10 (2015) e0124600.
- [26] S. Korkmaz, G. Zararsiz, D. Goksuluk, Drug/nondrug classification using support vector machines with various feature selection strategies, *Comput. Meth. Prog. Bio.* 117 (2014) 51–60.
- [27] Z. Ozdemir, A. Karakurt, U. Calis, S. Günel, S. Isik, Z. Sibel Sahin, S. Dalkara, Synthesis, anticonvulsant and antimicrobial activities of some new [1-(2-naphthyl)-2-(pyrazol-1-yl) ethanone] oxime ethers, *Med. Chem.* 11 (2015) 41–49.
- [28] W.A. Catterall, From ionic currents to molecular mechanisms: the structure and function of voltage-gated sodium channels, *Neuron* 26 (2000) 13–25.
- [29] E. Sigel, M.E. Steinmann, Structure, function, and modulation of GABA_A receptors, *J. Biol. Chem.* 287 (2012) 40224–40231.
- [30] M. Mantegazza, G. Curia, G. Biagini, D.S. Ragsdale, M. Avoli, Voltage-gated sodium channels as therapeutic targets in epilepsy and other neurological disorders, *Lancet Neurol.* 9 (2010) 413–424.
- [31] G.M. Lipkind, H.A. Fozzard, Molecular modeling of local anesthetic drug binding by voltage-gated sodium channels, *Mol. Pharmacol.* 68 (2005) 1611–1622.
- [32] D.S. Ragsdale, J.C. McPhee, T. Scheuer, W.A. Catterall, Molecular determinants of state-dependent block of Na⁺ channels by local anesthetics, *Science* 265 (1994) 1724–1728.
- [33] D.S. Ragsdale, J.C. McPhee, T. Scheuer, W.A. Catterall, Common molecular determinants of local anesthetic, antiarrhythmic, and anticonvulsant block of voltage-gated Na⁺ channels, *Proc. Natl. Acad. Sci. U. S. A.* 93 (1996) 9270–9275.
- [34] V. Yarov-Yarovoy, J. Brown, E.M. Sharp, J.J. Clare, T. Scheuer, W.A. Catterall, Molecular determinants of voltage-dependent gating and binding of pore-blocking drugs in transmembrane segment IIIIS6 of the Na⁺ channel α subunit, *J. Biol. Chem.* 276 (2001) 20–27.
- [35] R.A. Friesner, J.L. Banks, R.B. Murphy, T.A. Halgren, J.J. Klicic, D.T. Mainz, M.P. Repasky, E.H. Knoll, M. Shelley, J.K. Perry, Glide: a new approach for rapid, accurate docking and scoring. 1. Method and assessment of docking accuracy, *J. Med. Chem.* 47 (2004) 1739–1749.
- [36] R.A. Friesner, R.B. Murphy, M.P. Repasky, L.L. Frye, J.R. Greenwood, T.A. Halgren, P.C. Sanschagrin, D.T. Mainz, Extra precision glide: docking and scoring incorporating a model of hydrophobic enclosure for protein-ligand complexes, *J. Med. Chem.* 49 (2006) 6177–6196.
- [37] T.A. Halgren, R.B. Murphy, R.A. Friesner, H.S. Beard, L.L. Frye, W.T. Pollard, J.L. Banks, Glide: a new approach for rapid, accurate docking and scoring. 2. Enrichment factors in database screening, *J. Med. Chem.* 47 (2004) 1750–1759.
- [38] G.B. Smith, R.W. Olsen, Functional domains of GABA_A receptors, *Trends Pharmacol. Sci.* 16 (1995) 162–168.
- [39] D. Berezhnoy, Y. Nyfeler, A. Gonthier, H. Schwob, M. Goeldner, E. Sigel, On the benzodiazepine binding pocket in GABA_A receptors, *J. Biol. Chem.* 279 (2004) 3160–3168.
- [40] M. Davies, A.N. Bateson, S.M. Dunn, Structural requirements for ligand interactions at the benzodiazepine recognition site of the GABA_A receptor, *J. Neurochem.* 70 (1998) 2188–2194.
- [41] P.B. Wingrove, P. Safo, L. Wheat, S.A. Thompson, K.A. Wafford, P.J. Whiting, Mechanism of α -subunit selectivity of benzodiazepine pharmacology at γ -aminobutyric acid type A receptors, *Eur. J. Pharmacol.* 437 (2002) 31–39.
- [42] A. Buhr, R. Baur, E. Sigel, Subtle changes in residue 77 of the γ subunit of $\alpha 1\beta 2\gamma 2$ GABA_A receptors drastically alter the affinity for ligands of the benzodiazepine binding site, *J. Biol. Chem.* 272 (1997) 11799–11804.
- [43] P.B. Wingrove, S.A. Thompson, K.A. Wafford, P.J. Whiting, Key amino acids in the γ subunit of the γ -aminobutyric acid_A receptor that determine ligand binding and modulation at the benzodiazepine site, *Mol. Pharmacol.* 52 (1997) 874–881.
- [44] E. Sigel, M.T. Schaerer, A. Buhr, R. Baur, The benzodiazepine binding pocket of recombinant $\alpha 1\beta 2\gamma 2$ γ -aminobutyric acid_A receptors: relative orientation of ligands and amino acid side chains, *Mol. Pharmacol.* 54 (1998) 1097–1105.
- [45] K.R. Tan, R. Baur, A. Gonthier, M. Goeldner, E. Sigel, Two neighboring residues of loop A of the $\alpha 1$ subunit point towards the benzodiazepine binding site of GABA_A receptors, *FEBS Lett.* 581 (2007) 4718–4722.
- [46] S.M. Hanson, E.V. Morlock, K.A. Satyshur, C. Czajkowski, Structural requirements for eszopiclone and zolpidem binding to the γ -aminobutyric acid type-A (GABA_A) receptor are different, *J. Med. Chem.* 51 (2008) 7243–7252.
- [47] K.R. Tan, A. Gonthier, R. Baur, M. Ernst, M. Goeldner, E. Sigel, Proximity-accelerated chemical coupling reaction in the benzodiazepine-binding site of γ -aminobutyric acid type A receptors superposition of different allosteric modulators, *J. Biol. Chem.* 282 (2007) 26316–26325.
- [48] K.R. Tan, R. Baur, S. Charon, M. Goeldner, E. Sigel, Relative positioning of diazepam in the benzodiazepine-binding-pocket of GABA_A receptors, *J. Neurochem.* 111 (2009) 1264–1273.
- [49] A. Buhr, M.T. Schaerer, R. Baur, E. Sigel, Residues at positions 206 and 209 of the $\alpha 1$ subunit of γ -aminobutyric acid_A receptors influence affinities for benzodiazepine binding site ligands, *Mol. Pharmacol.* 52 (1997) 676–682.
- [50] M.T. Schaerer, A. Buhr, R. Baur, E. Sigel, Amino acid residue 200 on the $\alpha 1$ subunit of GABA_A receptors affects the interaction with selected benzodiazepine binding site ligands, *Eur. J. Pharmacol.* 354 (1998) 283–287.
- [51] R. Krall, J. Penry, B. White, H. Kupferberg, E. Swinyard, Antiepileptic drug development: II. Anticonvulsant drug screening, *Epilepsia* 19 (1978) 409–428.
- [52] J.L. Banks, H.S. Beard, Y. Cao, A.E. Cho, W. Damm, R. Farid, A.K. Felts, T.A. Halgren, D.T. Mainz, J.R. Maple, Integrated modeling program, applied chemical theory (IMPACT), *J. Comput. Chem.* 26 (2005) 1752–1780.
- [53] Rigaku, CrystalClear, Rigaku Corporation, Tokyo, Japan, 2014.
- [54] M.C. Burla, R. Caliandro, M. Camalli, B. Carrozzini, G.L. Cascarano, C. Giacovazzo, M. Mallamo, A. Mazzone, G. Polidori, R. Spagna, SIR2011: a new package for crystal structure determination and refinement, *J. Appl. Crystallogr.* 45 (2012) 357–361.
- [55] G.M. Sheldrick, A short history of SHELX, *Acta Crystallogr. Sect. A* 64 (2008) 112–122.